Published in final edited form as:

Muscle Nerve. 2017 March ; 55(3): 384–392. doi:10.1002/mus.25227.

Reduced skeletal muscle satellite cell number alters muscle morphology after chronic stretch but allows limited serial sarcomere addition

Matthew C. Kinney, MD[1], **Sudarshan Dayanidhi, PT, PhD**[1,2], **Peter B. Dykstra, BS**[3], **John J. McCarthy, PhD**[4], **Charlotte A. Peterson, PhD**[5], and **Richard L. Lieber, PhD**[1,2,3,*]

[1]Department of Orthopaedic Surgery, University of California, San Diego, CA, USA

[2]Department of Veterans Affairs Medical Center, San Diego, CA, USA

[3]Department of Bioengineering, University of California, San Diego, CA, USA

[4]Department of Physiology, University of Kentucky, Lexington, KY, USA

[5]Department of Rehabilitation Sciences, University of Kentucky, Lexington, KY, USA

Abstract

Introduction—Muscles add sarcomeres in response to stretch, presumably to maintain optimal sarcomere length. Clinical evidence from patients with cerebral palsy (CP), who have both decreased serial sarcomere number and reduced satellite cells (SCs), suggests a hypothesis that SCs may be involved in sarcomere addition.

Methods—A transgenic Pax7-DTA mouse model underwent conditional SC depletion, and their soleii were then stretch-immobilized to assess their capacity for sarcomere addition. Muscle architecture, morphology, and extra-cellular matrix (ECM) changes were also evaluated.

Results—Mice in the SC-reduced group achieved normal serial sarcomere addition in response to stretch. However, muscle fiber cross-sectional area was significantly smaller and was associated with hypertrophic extra-cellular matrix (ECM) changes, consistent with fibrosis.

Discussion—While a reduced SC population does not hinder serial sarcomere addition, SCs do play a role in muscle adaptation to chronic stretch that involves maintenance of both fiber cross-sectional area and ECM structure.

Keywords

satellite cells; sarcomere addition; chronic stretch; cerebral palsy; skeletal muscles; fibrosis

*Corresponding Author: Richard L. Lieber, PhD, Rehabilitation Institute of Chicago, 345 E. Superior Drive, Chicago, IL 60611, Tel.: +1 312 238 6260; fax: +1 312 238 1392. rlieber@ric.org (R.L. Lieber).

Disclosures: None of the authors have any conflict of interest or financial disclosures related to this work.

Introduction

Skeletal muscle undergoes remarkable adaptation to extrinsically-imposed length changes in order to regulate force-production capacity. The most important example of this phenomenon is serial sarcomere addition during longitudinal growth due to external stretch imposed by growing bone[1]. This basic process not only underlies postnatal longitudinal muscle growth[1] but also occurs in response to many other stretch-inducing stimuli, including chronic immobilization[2,3], surgical tensioning[4], and even distraction osteogenesis[5]. The plasticity of serial sarcomere number allows restoration of force generation in as little as 2 weeks after perturbation[6,7,1–3].

Despite general acceptance of the fact that sarcomerogenesis occurs in adult skeletal muscle, the cellular mechanisms that underlie this adaptive process are poorly understood. One hypothesis is that satellite cells, i.e. resident skeletal muscle stem cells[8], are involved in the sarcomere addition response to chronic muscle length change. Satellite cells (SCs) have been shown to be indispensible mediators of muscle growth during periods of postnatal development and regeneration following injury[9–12]. Specifically, they serve as the source of new myonuclei and myoblasts during muscle growth and repair[13–16].

While no studies to date have directly evaluated the role that SCs play in the muscle response to chronic stretch, there are observations from the cerebral palsy (CP) literature that suggest that they may be involved in the process of serial sarcomere addition. Spastic CP is characterized by impaired longitudinal muscle growth, persistent resistance to muscle stretch, and associated contracture formation[17]. CP patients have significantly longer sarcomere lengths[18–20], reduced serial sarcomere number[19], reduced myofiber area[20], and weakness[21] compared to their typically-developing counterparts, which suggests impairment in the ability to add serial sarcomeres. A pertinent point is that children with CP have a decreased number of SCs within contractured muscles, approximately 40% of expected[22,23]. These 2 findings, decreased SC number and altered sarcomere number, lead to the provocative suggestion that SCs may be responsible for mediating sarcomere addition in response to muscle length change.

In this study, we test this suggestion directly. To do this, we utilized a transgenic mouse model[24] that permits conditional SC ablation. We hypothesized that, after SC depletion, chronically-stretched muscles would be unable to add sarcomeres in series, leading to pathological muscle changes.

Materials and methods

Animal Subjects

Experiments were performed on 2 groups of mixed-gender young adult mice: wild-type C57BL/6 (N=7, aged 8 weeks; The Jackson Laboratory, Bar Harbor, ME, USA) and Pax7CreER/+;Rosa26DTA/+, referred to here as Pax7-DTA (N=18, aged 8 weeks)[24]. They were divided into 3 groups: wild-type (WT) control group (N=7, 3 male, negative control), Pax7-DTA control group (N=6, 4 male, treatment control), and Pax7-DTA treatment group (N=10, 6 male). Pax7CreER/+;Rosa26DTA/+ mice undergo ablation/reduction of their

satellite cell number by diphtheria toxin mediated only by treatment with tamoxifen but not with a vehicle control[24]. Mice were housed in a temperature- and humidity-controlled environment and maintained on a 12:12 hour light-dark cycle with food and water *ad libitum*. All animal procedures were conducted in accordance with institutional guidelines for care and use of laboratory animals as approved by the Animal Care and Use Committee of the University of California.

Satellite Cell Ablation

Wild-type control group and Pax7-DTA treatment group were administered tamoxifen (2 mg/day, dissolved in 10% ethanol in peanut oil; MP Biomedicals, Solon, OH, USA), while the Pax7-DTA control group was administered vehicle (10% ethanol in peanut oil) treatment via oral gavage for 5 consecutive days. A 10-day washout period was implemented prior to casting.

Hindlimb Immobilization

The right hindlimb of each mouse was immobilized in maximal dorsiflexion for 14 days by wrapping extra-fast setting plaster strips (BSN medical, Rutherford College, NC, USA) over a layer of Webril undercast padding (Covidien, Mansfield, MA USA) secured with a self-adherent bandage (3M, St. Paul, MN, USA), resulting in plantarflexor stretch and dorsiflexor shortening[25]. The contralateral hindlimb of each animal was not casted and served as an internal control. Casts were inspected daily for fraying or loosening and were repaired or replaced if their integrity was compromised. Casting and cast repairs were performed with mice anesthetized via inhalation of 2% isoflurane (Butler Schein, Dublin, OH, USA) delivered by an Ohmeda anesthesia system (model VMA; UK). Most mice were anesthetized 1–2 times during the experimental period.

Muscle Harvesting and Fixation

Prior to sacrifice, mice were anesthetized, and the casts were removed to leave the under-layer of webril and self-adherent bandage in place to maintain the immobilized joint angle. A radiograph of the casted hindlimb quantified dorsiflexion angle. Mean ankle joint angle was 59.5±3.7° (mean± SEM, N=10) of dorsiflexion from neutral for the experiment group, 66.3±1.8° (N=7) for the tamoxifen-treated wild-type control, and 68.3±3.6° (N=8) for the vehicle-treated Pax7-DTA control (positive values represent dorsiflexion).

Mice were then sacrificed under anesthesia by cervical dislocation. Each hindlimb was skinned and transected below the hip. Soleus muscle length was measured *in vivo* with the ankle in neutral. Tibialis anterior (TA), extensor digitorum longus (EDL), and soleus muscles were then carefully dissected from the hindlimb, and mass (M) was obtained by blotting muscles dry prior to weighing. Muscles were subsequently divided longitudinally to provide specimens for fixation or freezing. In addition, gastrocnemius and quadriceps muscles were removed to quantify satellite cell number by flow cytometry.

Muscle specimens designated for fixation were pinned at *in vivo* length (as measured above for soleus, estimated for TA/EDL) and fixed for 48 hours in low-odor 10% formalin (Fisher Scientific, Fair Lawn, NJ, USA). After fixation, muscles were rinsed 3 times in phosphate-

buffered saline (PBS) to remove residual fixative and stored in PBS for subsequent analysis. Muscle specimens designated for immunohistochemistry were pinned at *in vivo* length, flash frozen in liquid-nitrogen cooled isopentane, and stored at −80° for subsequent analysis.

Flow Cytometry

Quadriceps and gastrocnemius muscles from 8 Pax7-DTA mice (n=4 per treatment group) were utilized to quantify SC ablation due to tamoxifen administration. Previously used standard procedures for flow cytometry were adapted and utilized [24,22]. Briefly, immediately after harvest, muscles were placed in 15ml centrifuge tubes containing digestion buffer. They were incubated at 37°C and mechanically disrupted with forceps. The cell suspension was then filtered with a 40μm mesh. The mixture was centrifuged at 1300 rpm at 4°C for 10 mins, supernatant was discarded, and the pellet containing the mononuclear cells was resuspended in 1 ml fluorescence-activated cell sorting (FACS) buffer [1 mM Ethylenediaminetetraacetic acid (EDTA), 2.5% goat serum in phosphate-buffered saline (PBS), pH 7.4]. Fluorophore conjugated antibodies for specific markers for SCs, endothelial cells, and inflammatory cells were used for each of the samples: α7-integrin (Ablab, 1:200), CD31 (eBiosciences, 1:200), CD45 (eBiosciences, 1:200), respectively. An unconjugated antibody for NCAM (BD Biosciences, 1:200) was used along with a secondary fluorescent antibody (Goat anti-mouse Alexafluor 488, Invitrogen). Unstained controls and gating [Fluorescence minus one (FMO)] controls were used to ensure appropriateness of labeling.

Flow cytometry was performed using a FACS Canto (BD Biosciences, San Jose, CA, USA) instrument. PE fluorochromes were used for α7-integrin and NCAM, Pacific Blue for CD31 and CD45, and data for 60,000–100,000 cells/sample were obtained. Gating to exclude cellular debris and analysis was performed using FlowJo software v10. SCs were identified as $\alpha7\text{-integrin}^{+}/\text{NCAM}^{+}/\text{CD31}^{-}/\text{CD45}^{-}$ cells. FMO controls ($\alpha7\text{-integrin}^{-}/\text{NCAM}^{-}/\text{CD31}^{+}/\text{CD45}^{+}$) were used to ensure the specificity of gating for SC.

Muscle Architecture/Serial Sarcomere Number Measurements

Methods for architecture were modified from the protocol previously described in detail[26]. Briefly, fixed specimen muscle length was measured from the origin of the most proximal fibers to the insertion of the most distal fibers using digital calipers under a dissecting microscope. Muscles were then partially digested in 15% H_2SO_4 for 30 minutes to facilitate fiber dissection.

Multiple fiber bundles (3–6, composed of ~10 fibers each) were then dissected from muscles, and a digital caliper was used under the dissecting scope to measure fiber length. Fiber length was measured from 3 fiber bundles whenever possible (in a very small number of specimens (6 out of 135) there was insufficient tissue available, and only 2 measurements were made) and were averaged to provide mean fiber length (L_f) for each sample. Regional differences in the muscle have previously been shown to be insignificant[25], and were not considered.

Physiological cross-sectional area (PCSA) was calculated using the standard equation[27]:

$$\mathrm{PCSA}=M\cos\theta/\rho L_f \quad (1)$$

Literature values for pennation angles (θ) of the TA, EDL, and soleus[26], and muscle density (ρ, g/mm^3)[28] were used, and values for mass (M; g) and fiber length (L_f; mm) were measured directly. Muscle fiber lengths were normalized to a resting sarcomere length of 2.5 μm to permit comparisons among groups[29].

Serial sarcomere number (SN) was determined using the standard equation:

$$\mathrm{SN}=L_f/\mathrm{L_s} \quad (2)$$

Sarcomere length measurement (L_s) was initially attempted using the classic laser diffraction method[30]. However, due to the significant amount of derangement encountered in tamoxifen-treated Pax7-DTA mice, clear laser diffraction patterns could not be obtained. Sarcomere lengths were therefore measured optically using bright-field microscopy at 40X magnification (Leica DM3000, Buffalo Grove, IL, USA). The distance between 10–15 serial Z-bands representative of each sample was measured using the computerized caliper and dividing by the corresponding number of sarcomeres to determine mean sarcomere length for each bundle. Measurements were made on 3–5 bundles and were averaged to provide a mean sarcomere length for the muscle. Sarcomere number was then calculated by dividing the mean fiber length by the mean sarcomere length (Equation 2).

Muscle Histology and Immunohistochemistry

Serial cross-sections (10μm) of flash-frozen soleus muscles embedded in optimal cutting temperature (OCT) compound were created on a cryostat at −25°C (Microm HM500, Walldorf, Germany). Slides were stored at −20°C until the histology or immunohistochemistry protocols. Standardized protocols for hematoxylin and eosin (H&E) staining were used to evaluate general muscle morphology. For immunohistochemistry, slides were washed with PBS, then covered with a blocking solution (2% BSA, 5% FBS, 0.2% Triton X-100, 2% goat serum, 1xPBS) for 30 minutes. A primary antibody (Laminin 9393, rabbit polyclonal, Sigma, St. Louis, MI, USA) and a secondary antibody for laminin (Alexafluor 488 goat anti-rabbit IgG, Invitrogen) were utilized. A fluorescent mounting medium containing 4′, 6-diamidino-2-phenylindole (DAPI) to stain for nuclei was used, and slides were sealed with a cover slip. Muscle fiber area was calculated from laminin labeled sections for at least 150 myofibers per sample using ImageJ (NIH, Bethesda, MD, USA) as described previously[31].

The fraction of the cross-section occupied by muscle fibers (i.e., muscle area fraction) was calculated from soleus H&E stained sections using ImageJ (NIH, Bethesda, MD, USA). Images of 3–4 sections per specimen were obtained under 10X objective. Color thresholding based on hue and saturation of the H&E stained sections was used to differentiate the muscle region, stained pink, from the non-muscle region, such as extracellular matrix, stained white.

Muscle area measurements were then normalized to the area of the whole tissue section (100%), which we refer to as muscle area fraction.

Statistical Analysis

SCs were expressed as percentage of mononuclear cells for both tamoxifen and vehicle groups. Samples in the tamoxifen group were normalized to the average value of the vehicle group as the measure of SC knockdown. One-way analysis of variance (ANOVA) was used to compare percentage of SCs between groups. Significance level (α) for all tests was set to 0.05. Two-way ANOVA was used to compare mean sarcomere number between immobilized and non-immobilized hindlimbs and to compare serial sarcomere numbers between the 3 treatment groups along with multiple-comparisons using Sidak *post-hoc* tests. A correlation was performed between SC number, quantified by FACS and sarcomere number to evaluate whether the percentage of SCs affected sarcomere addition. PCSA differences between limbs were also assessed using the Student *t*-test (Prism 6.0d; GraphPad Software, Inc., La Jolla, CA, USA). *A priori* power analysis was performed and confirmed that 6 animals per group would provide sufficient experimental power to detect a 20% serial sarcomere number change. Muscle area fractions were compared between tamoxifen and vehicle groups (n=5–6 per group) using a 1-way ANOVA. Average myofiber area was compared between the 2 groups using a 1-way ANOVA.

Results

Quantification of SC number was performed at the time of muscle harvest (Fig. 1A), and revealed that an average of 0.81± 0.18% of all mononuclear cells in the tamoxifen-treated Pax7-DTA group were α7-integrin^{+}/NCAM^{+}/CD31^{-}/CD45^{-} SCs compared to 2.31± 0.39% of the vehicle-treated Pax7-DTA cohort (Figs. 1B, 1C). This represented a statistically significant 65% SC reduction in the treatment group (P<0.05).

With confirmation of SC knockdown, serial sarcomere number was then calculated for treatment and experimental groups. Importantly, and unexpectedly, there was no apparent inhibition of serial sarcomere addition in the SC knockdown muscle. Two-way ANOVA revealed a main effect for both limb and treatment groups (P<0.01) with no interaction. *Post-hoc* multiple comparisons between groups in sides, i.e. casted vs. uncasted, revealed, as predicted, that the soleus muscles in the control groups (Fig. 2A, left and right panels) added sarcomeres in response to stretch (WT: 3562±347 vs. 2992±415, Vehicle: 3185±440 vs. 2459±263). However, the SC depleted group (Fig. 2A, center panel) also added sarcomeres in a statistically-significant manner (2903±434 vs. 2408±361), indicating that serial sarcomerogenesis was not affected by decreased SC number. A difference in serial sarcomere number between the Pax7-DTA mice and control C57BL/6 mice was observed on a 2-way ANOVA (P<0.01; Fig. 2A black bars). We attributed this result to differences in mouse strain. *Post-hoc* multiple comparisons showed that the differences between the treatment groups were only between the WT and the tamoxifen treated groups for both the casted and uncasted sides but not between the control groups, i.e., WT and vehicle treated mice. No significant correlation was found between serial sarcomere addition and decreased SC number (P>0.5, r^2=0.03). Shortening-induced sarcomere loss was also unaffected by SC

depletion. The tibialis anterior (TA) muscle, an antagonist to the soleus, showed a significant decrease in sarcomere number after immobilization-induced shortening, the magnitude of which was similar among groups (Fig. 2B, WT: 2951±344 vs. 3396±227, Vehicle: 2707±344 vs. 3153±200, Tamoxifen: 2689±303 vs. 3265±349).

This finding was further verified by assessing sarcomere length to ensure that mice in each group appropriately compensated for chronic stretch. Consistent with previous findings, there were no significant side-to-side sarcomere length differences between any of the treatment groups for the TA, EDL, or soleus muscles. Tamoxifen-treated Pax7-DTA mice were equally adept at maintaining sarcomere length despite the absence of a full cohort of SC (Table 1).

Notably, there were significant differences in muscle mass between sides in TA and EDL muscles across all treatment groups, consistent with the expected atrophy in the dorsiflexor muscle groups. There was no significant difference in soleus muscle mass in any treatment cohort (Table 1). However, when evaluating PCSA (which takes into account the effects of mass and fiber length) there was a significant side-to-side difference in the soleus muscle across all groups. This is consistent with an expected finding of immobilization-induced atrophy. Taken together, the results from Table 1 and Figure 2 indicate that SC reduction did not inhibit the muscle's ability to adapt to chronic stretch/shortening by altering serial sarcomere number to maintain sarcomere length.

However, despite preservation of serial sarcomere number, SC depleted muscles contained important structural alterations in both the muscle fibers and the extracellular matrix. Differences in muscle morphology between the vehicle-treated (Fig. 3A, left panel) and tamoxifen-treated (Fig. 3A, right panel) Pax7-DTA mice were obvious. A large number (50–60%) of the stretched muscle fibers in both groups of Pax7-DTA showed centralized nuclei indicating that the process of serial sarcomere number addition mimics the regenerative process in other muscle models[32]. Compared to vehicle-treated controls, SC depleted muscle displayed mononuclear cell proliferation in the extracellular matrix consistent with fibrosis. Soleus muscle area fraction in casted tamoxifen-treated muscle was only 11 ± 6% compared to values of 69 ± 3% for casted vehicle-treated muscle and 66 ± 2% for uncasted tamoxifen-treated muscle (Fig. 3C, $P<0.01$). Furthermore, myofiber area was significantly decreased in SC depleted muscle (Fig. 3D, $P<0.05$). The tamoxifen-treated Pax7-DTA stretched soleus had a fiber area of only 263 ± 48 μm^2 compared to 1,396 ± 208 μm^2 on the uncasted side and 869 ± 263 μm^2 in the vehicle treated stretched solei (Fig. 3D). Sarcomere addition can be both in series, i.e. along the length of the fiber and in parallel, i.e. within the fiber cross-section. Fiber area is an indirect measure of sarcomeres in parallel, while serial sarcomere number is a measure of sarcomeres in series along the length of the fiber. These data suggest that while sarcomere addition observed in series, i.e. serial sarcomere number is permissible in the presence of reduced SC number, sarcomere addition in parallel, i.e. fiber size might be affected with reduced SC number.

Discussion

This study demonstrated that stretch-induced sarcomere adaptation is dependent on a full cohort of SCs. We used a SC conditional knockdown mouse model, reduced the SC to the same level seen in children with CP (30–40%), and induced sarcomerogenesis by stretching the soleus muscle in a position of dorsiflexion. While a reduced cohort, such as those seen in children with CP, is sufficient for some addition of sarcomeres, a full cohort is needed for optimal adaptation, specifically for maintaining myofiber area and regulating the extracellular matrix (ECM). Both myofiber area and muscle area fraction were dramatically reduced in the cohort with reduced SCs. Furthermore, a large percentage (~50%) of fibers in the vehicle group showed clear centralized nuclei, typically indicative of myofiber repair and regeneration[32]. This suggests that the process of sarcomere addition under conditions of chronic stretch may be a regenerative process, which requires participation by the SC, but this has not been demonstrated before. However this was seen only in a small percentage (~10%) of the fibers in the WT mice. Consequently the centralized nuclei might not be as indicative of stretch-induced regeneration as much as a Pax7-DTA transgenic mouse-specific response. In contrast to a regenerative process such as repair after injury for which SCs are indispensable [33] they are dispensable for conditions of hypertrophy [24] and re-growth from atrophy [34] with no loss of myonuclei during conditions of atrophy [35]. These findings, while unexpected based on our initial hypothesis, provide additional evidence that SC depletion may be either directly or indirectly (see below) associated with an improper regenerative response and inappropriate muscle adaptation.

The role of SCs in regulation of the extracellular matrix has recently been suggested in other models that require muscle adaptation to external stimuli. Murphy *et al.* demonstrated that interaction between SCs and fibroblasts are important for appropriate muscle regeneration after barium chloride injury[36]. More recently, Fry *et al.* showed that activated SCs are important regulators of ECM changes in response to muscle overload[37]. One proposed mechanism is that SC activation is associated with upregulation of interstitial collagenases, which allow ECM remodeling and SC migration[38,39]. These studies indicate that a major role of the SC may be to “manage” the response of the extracellular matrix to external stimuli, a finding strongly corroborated by our observation that reduction of SCs prevented appropriate ECM remodeling in response to chronic stretch.

From a clinical standpoint, this is a compelling discovery in light of the notable abnormalities seen in the pathologic muscles of patients with common muscle disorders. Compared with their typically-developing counterparts, the muscles of children with CP have increased collagen content, increased bundle passive stiffness, and qualitatively increased levels of ECM, consistent with muscle fibrosis[20]. As previously discussed, these contractured muscles also have considerable atrophy and significantly reduced SC number[22,23], providing evidence that a major role of SCs is to regulate the extracellular muscle environment. It is not clear why children with CP, who also have lower activity levels, have these ECM changes, develop contractures, or have reduced SC number. However without sufficient SC numbers, it appears as though this process of ECM regulation fails and results in the muscle contracture development. In support of this conjecture, other pathologic muscle conditions associated with marked fibrotic changes,

including Duchenne muscular dystrophy (DMD), are also associated with SC depletion. In biopsies from children with DMD there is strong evidence to suggest a decline and functionality of the satellite cells/muscle progenitors[40], and muscle fibrosis is common in children with DMD[41,42]. Additional studies must be performed, however, to determine whether contracture formation can be induced from a SC depleted model and to determine whether contracture development itself can result in the increased sarcomere length[18,20] observed in children with CP. Importantly, serial casting for up to 2 weeks at the maximal possible range of motion is commonly used for increasing joint excursion and presumably muscle fascicle length and serial sarcomere number in children with CP[43], who have reduced SC numbers. Consequently our results show that the adaptation in response to casting-induced stretch, in the presence of a reduced number of SCs might not be appropriate. This adds basic science information to the debate as to whether serial casting is beneficial for children with CP[44]. However the maximal ankle angle during serial casting in children with CP and our mouse model are different, and given the paucity of direct information in muscles of children with CP, this response to stretch may be different in those children.

The results of architectural changes in the stretched muscles in this experiment correlate closely with findings from other stretch-immobilization experiments in the literature. The 21% increase in soleus sarcomere number after 2 weeks of stretch is similar to the ~17% increase reported in the original study describing the phenomenon of sarcomerogenesis[2]. Furthermore, decreases in muscle mass and PCSA after prolonged immobilization have also been reported in other studies, consistent with muscle atrophy[25]. These findings provide validation for the approach used in this experiment.

It should be noted that using previously-described methods in our Pax7-DTA mouse model, we were able to obtain a statistically-significant 65% knockdown in SC number. This is a smaller reduction than was previously-reported[24], raising the possibility that remaining SCs compensated for depletion and were sufficient to allow for quantitatively-normal serial sarcomerogenesis. However, this incomplete knockdown of SC is similar to the SC number observed in muscle of children with CP, where SCs are depleted by 60–70%[22,23]. Thus, we believe that the findings we present are of clinical relevance despite incomplete SC depletion.

This study has important limitations. Due to size limitations with the use of the soleus, we quantified the SC number using flow cytometry with the quadriceps and gastrocnemius muscles. In this previously established transgenic mouse model the SC reduction should be systemic[45], and consequently the results observed in overall reduction between the vehicle control group and the tamoxifen treatment group should hold true for the soleus. Based on the significant phenotypic differences seen in experimental and control muscle tissues that were visible with light microscopy, it was not feasible to perform sarcomere length analysis in a truly blinded fashion. Furthermore, muscle architectural measurements may have been skewed by the presence of proximal and distal tendon samples which were included in the muscle mass and PCSA determination to allow proper pinning of the muscles at *in vivo* lengths. In addition, to have sufficient muscle tissue to perform both architectural studies and histologic sectioning, each studied muscle was divided longitudinally to provide 2

specimens for each muscle. This limited our ability to directly quantify total fiber number but not fiber size in each muscle. In addition, we only analyzed the muscles at the 14-day time point. Consequently our work is not informative of the timeline of development of fibrosis and pathological changes since we were unable to test intermediate time points. Due to practical consideration we used the contralateral leg as internal control per mouse rather than a truly non-manipulated control. However as we elaborate in our methods we used appropriate littermate controls as treatment control (i.e. tamoxifen vs. vehicle) and wild-type mice (treated with tamoxifen) as our negative control. There might be changes in the contralateral leg due to the cast, but this should not impact the serial sarcomere number, i.e. sarcomere number associated with the length of the muscle fascicle. In general, our mice are very mobile, and gait patterns are fairly normal. We and others have used this model extensively to study sarcomere adaptation to length changes[25,2,1]. Another important point, which is an ongoing debate in the field, is the translational capacity of using murine models to understand human disease and biology. SCs in mice and humans may differ in their phenotype and functionality[46], however murine transgenic models allow manipulation of conditions in a way that is currently not possible in humans. Finally, it is worth noting that SC numbers differ between genders and muscles[47], and consequently we used mixed gender groups in our 3 groups.

In summary, this study demonstrates that, while SC reduction does not preclude serial sarcomere addition in response to chronic stretch, it results in pathological changes in the muscle, including reduction of myofiber number, decreased muscle area fraction, and increased muscle fibrosis.

Acknowledgments

We appreciate the assistance of Dr. Simon Schenk with mouse treatment, Mary Esparza with muscle harvesting, and Dr. Gretchen Meyer with flow cytometry methods.

Funding

The authors acknowledge NIH grants P30AR061303 and HD050837 and Department of Veterans Affairs grant A9028-R for support. This research was also aided by a grant from the Orthopaedic Research and Education Foundation, with Funding Provided by Depuy Synthes Joint Reconstruction.

List of symbols and abbreviations

SC	Satellite cells
CP	Cerebral palsy
TA	Tibialis Anterior
EDL	Extensor Digitorum Longus

References

1. Williams PE, Goldspink G. Longitudinal growth of striated muscle fibres. Journal of cell science. 1971; 9(3):751–767. [PubMed: 5148015]
2. Williams PE, Goldspink G. The effect of immobilization on the longitudinal growth of striated muscle fibres. J Anat. 1973; 116(Pt 1):45–55. [PubMed: 4798240]

3. Williams PE, Goldspink G. Changes in sarcomere length and physiological properties in immobilized muscle. J Anat. 1978; 127(Pt 3):459–468. [PubMed: 744744]
4. Takahashi M, Ward SR, Marchuk LL, Frank CB, Lieber RL. Asynchronous muscle and tendon adaptation after surgical tensioning procedures. J Bone Joint Surg Am. 2010; 92(3):664–674. [PubMed: 20194325]
5. Boakes JL, Foran J, Ward SR, Lieber RL. Muscle adaptation by serial sarcomere addition 1 year after femoral lengthening. Clin Orthop Relat Res. 2007; 456:250–253. [PubMed: 17065842]
6. Tardieu C, Tabary JC, Tabary C, Huet de la Tour E. Comparison of the sarcomere number adaptation in young and adult animals. Influence of tendon adaptation. J Physiol (Paris). 1977; 73(8):1045–1055. [PubMed: 615249]
7. Tardieu G, Thuilleux G, Tardieu C, de la Tour EH. Long-term effects of surgical elongation of the tendo calcaneus in the normal cat. Dev Med Child Neurol. 1979; 21(1):83–94. [PubMed: 437387]
8. Mauro A. Satellite cell of skeletal muscle fibers. J Biophys Biochem Cytol. 1961; 9:493–495. [PubMed: 13768451]
9. Zammit PS, Partridge TA, Yablonka-Reuveni Z. The skeletal muscle satellite cell: the stem cell that came in from the cold. J Histochem Cytochem. 2006; 54(11):1177–1191. [PubMed: 16899758]
10. Oustanina S, Hause G, Braun T. Pax7 directs postnatal renewal and propagation of myogenic satellite cells but not their specification. Embo J. 2004; 23(16):3430–3439. [PubMed: 15282552]
11. Lepper C, Conway SJ, Fan CM. Adult satellite cells and embryonic muscle progenitors have distinct genetic requirements. Nature. 2009; 460(7255):627–631. [PubMed: 19554048]
12. Kuang S, Rudnicki MA. The emerging biology of satellite cells and their therapeutic potential. Trends Mol Med. 2008; 14(2):82–91. [PubMed: 18218339]
13. Moss FP, Leblond CP. Satellite cells as the source of nuclei in muscles of growing rats. The Anatomical record. 1971; 170(4):421–435. [PubMed: 5118594]
14. Macconnachie HF, Enesco M, Leblond CP. The Mode of Increase in the Number of Skeletal Muscle Nuclei in the Postnatal Rat. The American journal of anatomy. 1964; 114:245–253. [PubMed: 14131858]
15. Enesco M, Puddy D. Increase in the Number of Nuclei and Weight in Skeletal Muscle of Rats of Various Ages. The American journal of anatomy. 1964; 114:235–244. [PubMed: 14131857]
16. Snow MH. An autoradiographic study of satellite cell differentiation into regenerating myotubes following transplantation of muscles in young rats. Cell Tissue Res. 1978; 186(3):535–540. [PubMed: 627031]
17. Graham HK, Selber P. Musculoskeletal Aspects Of Cerebral Palsy. Journal of Bone & Joint Surgery, British Volume. 2003; 85-B(2):157–166.
18. Lieber RL, Friden J. Spasticity causes a fundamental rearrangement of muscle-joint interaction. Muscle & nerve. 2002; 25(2):265–270. [PubMed: 11870696]
19. Mathewson MA, Ward SR, Chambers HG, Lieber RL. High resolution muscle measurements provide insights into equinus contractures in patients with cerebral palsy. Journal of Orthopaedic Research. 2015; 33(1):33–39. [PubMed: 25242618]
20. Smith LR, Lee KS, Ward SR, Chambers HG, Lieber RL. Hamstring contractures in children with spastic cerebral palsy result from a stiffer extracellular matrix and increased in vivo sarcomere length. The Journal of physiology. 2011; 589(Pt 10):2625–2639. [PubMed: 21486759]
21. Mockford M, Caulton JM. The Pathophysiological Basis of Weakness in Children With Cerebral Palsy. Pediatric Physical Therapy. 2010; 22(2):222–233. [PubMed: 20473109]
22. Smith LR, Chambers HG, Lieber RL. Reduced satellite cell population may lead to contractures in children with cerebral palsy. Developmental Medicine & Child Neurology. 2013; 55(3):264–270. [PubMed: 23210987]
23. Dayanidhi S, Dykstra PB, Lyubasyuk V, McKay BR, Chambers HG, Lieber RL. Reduced satellite cell number in situ in muscular contractures from children with cerebral palsy. Journal of Orthopaedic Research. 2015; 33(7):1039–1045. [PubMed: 25732238]
24. McCarthy JJ, Mula J, Miyazaki M, Erfani R, Garrison K, Farooqui AB, Srikuea R, Lawson BA, Grimes B, Keller C, Van Zant G, Campbell KS, Esser KA, Dupont-Versteegden EE, Peterson CA. Effective fiber hypertrophy in satellite cell-depleted skeletal muscle. Development. 2011; 138(17):3657–3666. [PubMed: 21828094]

25. Shah SB, Peters D, Jordan KA, Milner DJ, Friden J, Capetanaki Y, et al. Sarcomere number regulation maintained after immobilization in desmin-null mouse skeletal muscle. Journal of Experimental Biology. 2001; 204(10):1703–1710. [PubMed: 11316490]
26. Burkholder TJ, Fingado B, Baron S, Lieber RL. Relationship between muscle fiber types and sizes and muscle architectural properties in the mouse hindlimb. J Morphol. 1994; 221(2):177–190. [PubMed: 7932768]
27. Powell PL, Roy RR, Kanim P, Bello MA, Edgerton VR. Predictability of skeletal muscle tension from architectural determinations in guinea pig hindlimbs. J Appl Physiol Respir Environ Exerc Physiol. 1984; 57(6):1715–1721. [PubMed: 6511546]
28. Mendez JKA. Density and composition of mammalian muscle. Metabolism. 1960; 9:184–188.
29. Burkholder TJ, Lieber RL. Sarcomere number adaptation after retinaculum transection in adult mice. The Journal of experimental biology. 1998; 201(Pt 3):309–316.
30. Lieber RL, Yeh Y, Baskin RJ. Sarcomere length determination using laser diffraction. Effect of beam and fiber diameter. Biophys J. 1984; 45(5):1007–1016. [PubMed: 6610443]
31. Minamoto VB, Hulst JB, Lim M, Peace WJ, Bremner SN, Ward SR, et al. Increased efficacy and decreased systemic-effects of botulinum toxin A injection after active or passive muscle manipulation. Developmental Medicine & Child Neurology. 2007; 49(12):907–914. [PubMed: 18039237]
32. Folker E, Baylies M. Nuclear Positioning in Muscle Development and Disease. Frontiers in physiology. 2013; 4
33. Lepper C, Partridge TA, Fan CM. An absolute requirement for Pax7-positive satellite cells in acute injury-induced skeletal muscle regeneration. Development. 2011; 138(17):3639–3646. [PubMed: 21828092]
34. Jackson JR, Mula J, Kirby TJ, Fry CS, Lee JD, Ubele MF, et al. Satellite cell depletion does not inhibit adult skeletal muscle regrowth following unloading-induced atrophy. American Journal of Physiology - Cell Physiology. 2012; 303(8):C854–C861. [PubMed: 22895262]
35. Bruusgaard JC, Gundersen K. In vivo time-lapse microscopy reveals no loss of murine myonuclei during weeks of muscle atrophy. The Journal of clinical investigation. 2008; 118(4):1450–1457. [PubMed: 18317591]
36. Murphy MM, Lawson JA, Mathew SJ, Hutcheson DA, Kardon G. Satellite cells, connective tissue fibroblasts and their interactions are crucial for muscle regeneration. Development. 2011; 138(17): 3625–3637. [PubMed: 21828091]
37. Fry CS, Lee JD, Jackson JR, Kirby TJ, Stasko SA, Liu H, et al. Regulation of the muscle fiber microenvironment by activated satellite cells during hypertrophy. Faseb J. 2014; 28(4):1654–1665. [PubMed: 24376025]
38. Pallafacchina G, Francois S, Regnault B, Czarny B, Dive V, Cumano A, et al. An adult tissue-specific stem cell in its niche: a gene profiling analysis of in vivo quiescent and activated muscle satellite cells. Stem Cell Res. 2010; 4(2):77–91. [PubMed: 19962952]
39. Nishimura T, Nakamura K, Kishioka Y, Kato-Mori Y, Wakamatsu J, Hattori A. Inhibition of matrix metalloproteinases suppresses the migration of skeletal muscle cells. J Muscle Res Cell Motil. 2008; 29(1):37–44. [PubMed: 18563597]
40. Blau HM, Webster C, Pavlath GK. Defective myoblasts identified in Duchenne muscular dystrophy. Proceedings of the National Academy of Sciences. 1983; 80(15):4856–4860.
41. Zhou L, Lu H. Targeting Fibrosis in Duchenne Muscular Dystrophy. Journal of Neuropathology & Experimental Neurology. 2010; 69(8):771–776. [PubMed: 20613637]
42. Kharraz Y, Guerra J, Pessina P, Serrano AL, Muñoz-Cánoves P. Understanding the Process of Fibrosis in Duchenne Muscular Dystrophy. BioMed Research International. 2014; 2014:11.
43. Blackmore AM, Boettcher-Hunt E, Jordan M, Chan MDY. A systematic review of the effects of casting on equinus in children with cerebral palsy: an evidence report of the AACPDM. Developmental Medicine & Child Neurology. 2007; 49(10):781–790. [PubMed: 17880650]
44. Gough M. Serial casting in cerebral palsy: panacea, placebo, or peril? Developmental Medicine & Child Neurology. 2007; 49(10):725–725. [PubMed: 17880639]

45. Fry CS, Lee JD, Mula J, Kirby TJ, Jackson JR, Liu F, et al. Inducible depletion of satellite cells in adult, sedentary mice impairs muscle regenerative capacity without affecting sarcopenia. Nat Med. 2015; 21(1):76–80. [PubMed: 25501907]

46. Boldrin L, Muntoni F, Morgan JE. Are human and mouse satellite cells really the same? Journal of Histochemistry & Cytochemistry. 2010; 58(11):941–955. [PubMed: 20644208]

47. Neal A, Boldrin L, Morgan JE. The Satellite Cell in Male and Female, Developing and adult mouse muscle: distinct stem cells for growth and regeneration. PLoS ONE. 2012; 7(5):e37950. [PubMed: 22662253]

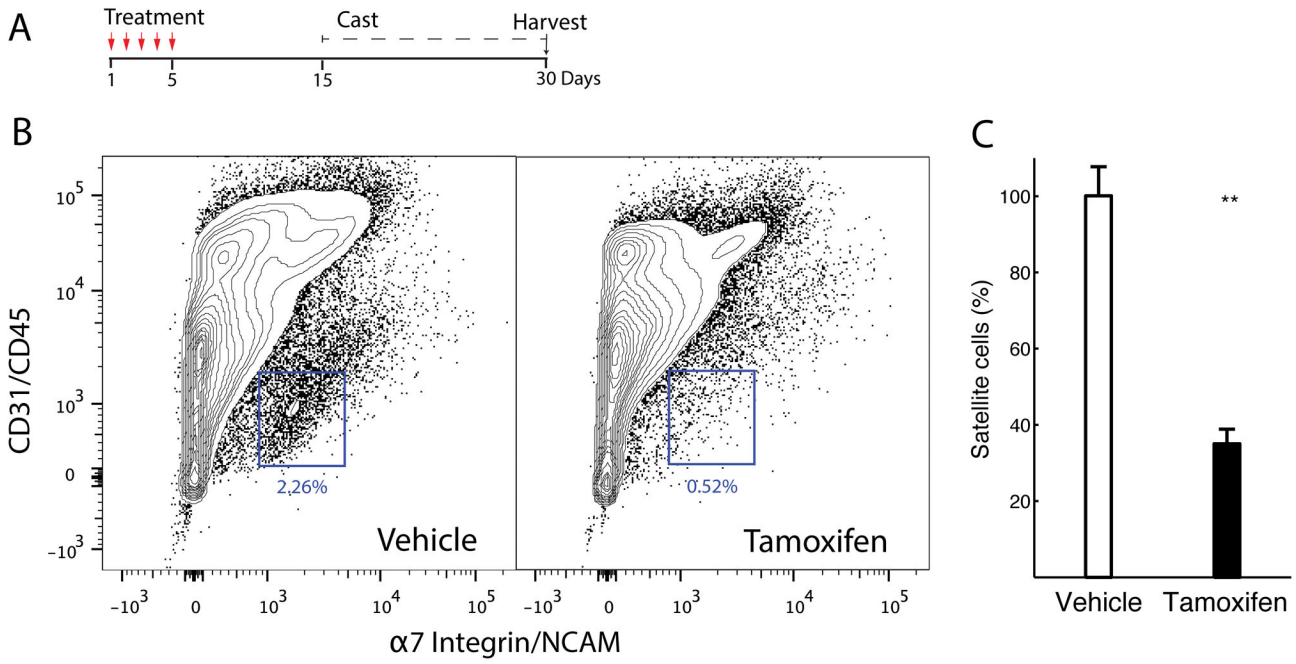

Fig. 1. Successful conditional ablation of satellite cells

(A) Timeline of experimental protocol indicating treatment either by oral gavage of tamoxifen or vehicle, followed by washout period, number of days casted, and day when the muscle was harvested. (B) Fluorescence-activated cell sorting (FACS) analysis from gastrocnemius and quadriceps muscles in treated mice confirmed satellite cell reduction, i.e., α7-integrin^{+}/NCAM^{+}/CD31^{-}/CD45^{-} cells in tamoxifen-treated Pax7-DTA muscles relative to vehicle-treated Pax7-DTA muscles (compare blue boxes, which display representative cell populations). Image is representative of 4 independent tests. (C) Quantification of FACS analysis shows an average 65% (range 58–78) reduction of satellite cells in tamoxifen-treated muscles compared with vehicle-treated muscles (n=4 per group, P<0.01, plotted as mean + SEM).

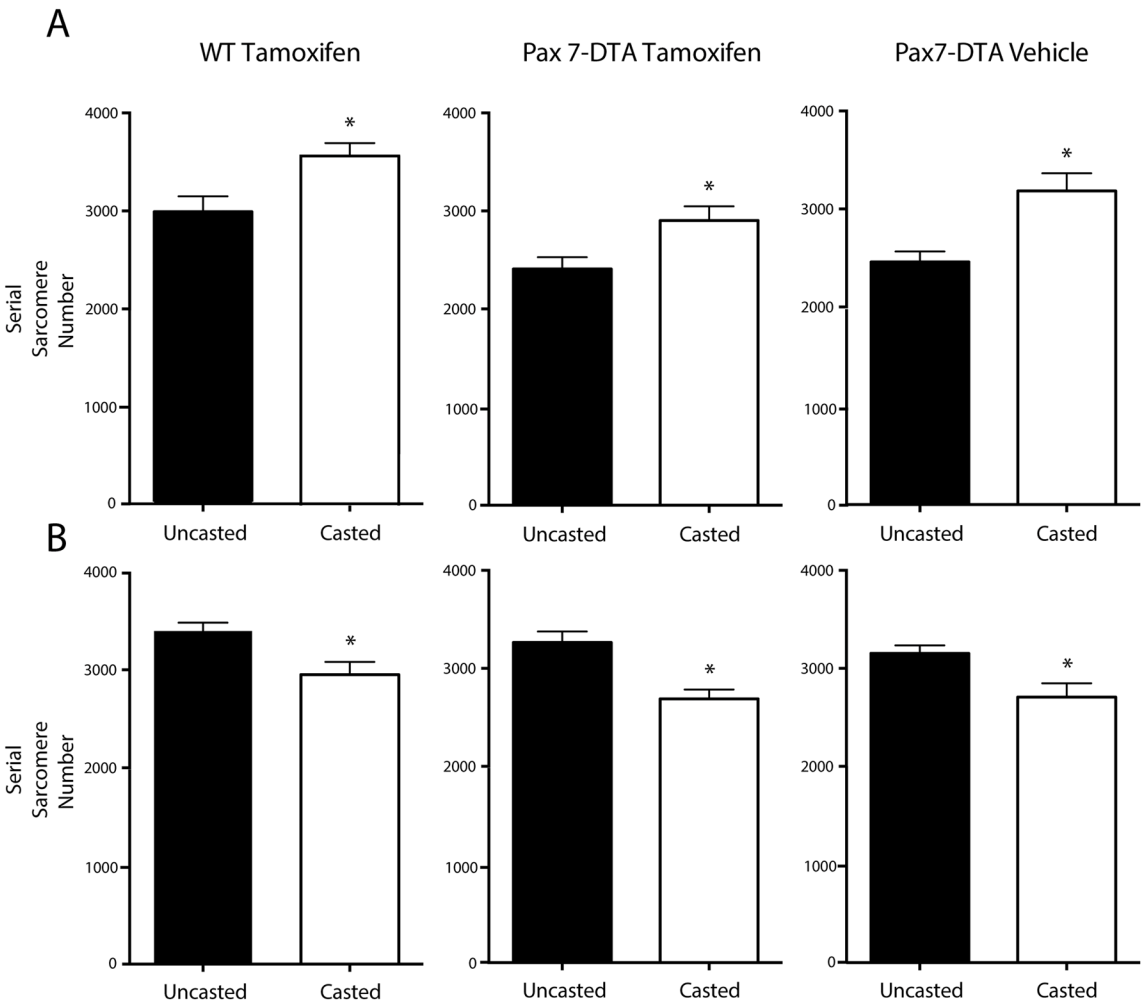

Fig. 2. Sarcomere number adaptation occurs after satellite-cell reduction

Serial sarcomere number addition in soleus (A) and subtraction in tibialis anterior (B) muscles from casted and uncasted hindlimbs of wild-type, tamoxifen-treated mice (tamoxifen control group); Pax7-DTA, tamoxifen-treated mice (experimental group); and Pax7-DTA, vehicle-treated mice (treatment control group). Data are plotted as mean + SEM (N=10 for experimental group, N=7–8 for control groups).* Statistically significant difference between casted and uncasted hindlimbs ($P<0.05$).

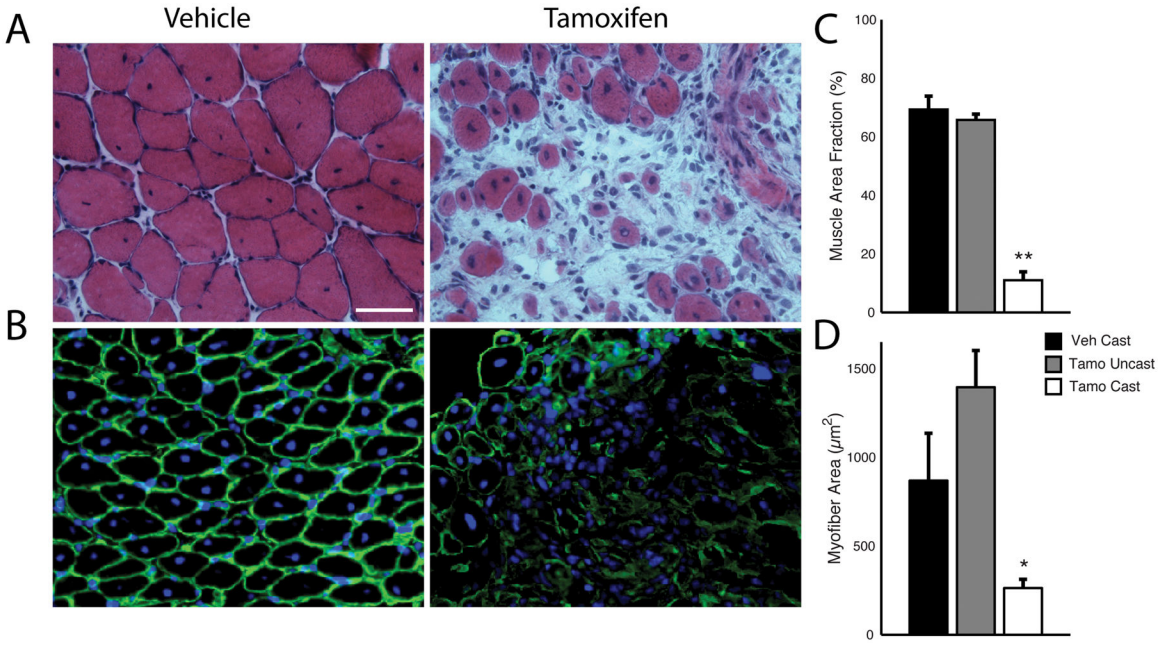

Fig. 3. Satellite cell depleted muscle is fibrotic with decreased muscle fiber sizes

(A) H&E stains of vehicle-treated Pax7-DTA soleus (left) and tamoxifen-treated Pax7-DTA soleus (right) on the cast side with a 20X objective (Scale bar = 50 μm). Images are representative of results from 5 independent samples per group. (B) Laminin antibody labeling of vehicle-treated Pax7-DTA soleus (left) and tamoxifen-treated Pax7-DTA soleus (right) on the cast side using a 10X objective (Scale bar = 100 μm, for all images). Displayed images are representative of 4–5 independent samples per group. (C) Quantification of percentage area of H&E stained sections of the soleus that was muscle tissue. (D) Quantification of soleus myofiber area calculated from laminin-labeled samples (n=4–5 per group). Data are represented as mean ± SEM. *statistically significant differences compared to uncasted sided and vehicle-treatment, $P<0.05$ (D) and **$P<0.01$ (C).

Table 1

Architectural changes in muscles from satellite-cell depleted and control mice

		Tamoxifen-Treated WT		Tamoxifen-Treated Pax7-DTA		Vehicle-Treated Pax7-DTA	
		Casted	**Uncasted**	**Casted**	**Uncasted**	**Casted**	**Uncasted**
Soleus	Mass (g)	9.11±3.65	10.8±2.46	9.03±2.55	10.9±2.27	7.90±294	9.02±2.19
	Raw Fiber Length (mm)	8.87±1.06	7.43±1.41	7.83±1.41	6.85±1.36	8.74±1.13	6.97±0.46 *
	PCSA (mm^2)	0.95±0.36	1.38±0.35 *	1.17±0.28	1.74±0.53 *	0.91±0.27	1.37±0.28 *
	Sarcomere Length (μm)	2.49±0.12 +	2.49±0.33 +	2.69±0.15	2.83±0.26	2.75±0.16	2.85±0.20
TA	Mass (g)	23.1±5.92	37.3±4.52 *	25.2±9.35	37.2±7.63 *	25.1±5.50	37.5±6.47 *
	Raw Fiber Length (mm)	6.22±0.79	7.56±1.04 *	6.33±0.90	7.21±0.76 *	5.98±0.62	7.04±0.74 *
	PCSA (mm^2)	2.90±0.60	4.11±0.64 *	3.45±1.11	4.22±0.67	3.52±1.05	4.40±0.63
	Sarcomere Length (μm)	2.11±0.17 +	2.23±0.26	2.35±0.23	2.22±0.20	2.22±0.12	2.23±0.21
EDL	Mass (g)	6.29±1.25	9.33±1.09 *	5.96±2.27	8.00±1.64 *	6.95±1.04	8.67±1.13 *
	Raw Fiber Length (mm)	5.52±0.87	7.03±1.33 *+	4.80±0.50	5.64±0.95 *	5.82±0.81 +	6.37±0.54
	PCSA (mm^2)	1.06±0.29	1.25±0.22	1.16±0.44	1.41±0.35	1.26±0.27	1.44±0.22
	Sarcomere Length (μm)	2.48±0.29	2.48±0.15	2.51±0.27	2.61±0.20	2.78±0.39	2.83±0.28
	Sarcomere Number	2242±356 +	2832±445 *+	1922±192	2154±284	2159±212 +	2265±236

Values are listed as mean ± SD for tamoxifen-treated WT (N=7) and vehicle-treated Pax7-DTA groups (N=6), and for tamoxifen-treated Pax7-DTA group (N=10). For measurement of physiologic cross-sectional area (PCSA), raw fiber length was normalized to a resting sarcomere length of 2.5μm.

* significant difference (P<0.05) between the casted limb and the uncasted limb.

+ significant difference (P<0.05) between the experimental and control groups.